Theoretical Study of the Phototoxicity of Naproxen and the Active Form of Nabumetone

Klefah A. K. Musa and Leif A. Eriksson*

Department of Natural Sciences and Örebro Life Science Center, Örebro University, 701 82 Örebro, Sweden

Received: June 25, 2008

Density functional theory using the hybrid functional B3LYP has been employed in order to study the mechanisms of photoinduced decomposition of the closely related nonsteroidal anti-inflammatory drugs naproxen (NP) and 6-methoxy-2-naphthylacetic acid (MNAA; the active form of nabumetone). The photochemical properties and computed energies of various species obtained in this study show that both drugs dominate in their deprotonated forms at physiological pH. The deprotonated acids are unable to decarboxylate from their excited singlets; instead, they decarboxylate from their first excited triplet states with high efficiency, overcoming energy barriers less than 3 and 1 kcal/mol for MNAA and NP, respectively. The ultraviolet and visible spectra of the neutral, deprotonated, and decarboxylated moieties of MNAA and NP are more-or-less similar but with higher probabilites (oscillator strength) for the latter. This fact, as well as the higher reactivity of NP, is explained in terms of the electron-donating effect of the additional methyl group present in NP. Singlet oxygen, superoxide radical anion, and corresponding peroxyl radical species are expected to be formed in different steps throughout the proposed photodegradation pathways of both drugs, which give rise to their effects on biomolecules, for example, lipid peroxidation.

Introduction

Most drugs are subjected to some type of photochemical decomposition leading to what is known as drug phototoxicity—immediate or delayed inflammatory reaction reflecting cellular damage produced as a result of a photochemical reaction between the drug and radiation. Once photodegradation has occurred, the medicinal preparations no longer have the desired pharmacological potency and may, in addition, contain harmful decomposition photoproducts. Of equal importance, a drug may undergo a variety of unwanted chemical or photochemical reactions once admitted. Questions pertaining to drug stability and fate during metabolism are, hence, of paramount importance in drug development and drug delivery.[1]

Naproxen (NP) and Nabumetone (NB) (Figure 1) are nonsteroidal anti-inflammatory drugs (NSAIDs). Chemically, NP belongs to the 2-arylpropionic acid family, whereas NB is found in the 2,6-disubstituted naphthylalkanone class. The latter is a prodrug metabolized to the active metabolite, 6-methoxy-2-naphthylacetic acid (MNAA). Both NP and MNAA act by inhibition of cyclo-oxygenase enzymes, have anti-inflammatory as well as analgesic properties, and are used in the treatment of rheumatoid arthritis, osteoarthritis, and other musculoskeletal disorders.[1−5] Patients taking nabumetone display significantly lower risk of hospitalization for peptic ulcer disease by preventing gastric damage accompanied by the reduction of neutrophil infilitration into the gastric mucosa.[6] Interestingly, such an effect is, however, not observed with its metabolite MNAA.[7]

The three major metabolic pathways of nabumetone are O-demethylation, reduction to alcohol derivatives, or oxidative cleavage of the side-chain to yield acetic acid derivatives.[3] The transformation of nabumetone into the pharmacologically active form MNAA (the latter of the metabolic pathways), occurs by extensive first-pass metabolism.[1,3,8,9] Nabumetone, which has an elimination half-life of approximately 24 h,[10] causes a moderate increase in blood pressure, without change in biological diurnal variation,[11] and has been associated with photosensitivity and skin lesions arising in photoexposed areas in patients treated with the drug.[12,13]

MNAA does not undergo enterohepatic recirculation (the process by which a drug is reabsorbed in the gastrointestinal tract after biliary excretion).[1] Irradiation studies have shown that the metabolite MNAA is photolabile, giving two major compounds in aerated phosphate buffered saline (PBS) solution: 6-methoxynaphthaldehyde and the corresponding alcohol derivative, with the former formed through oxidative photodegradation. This process has been described for related molecules to proceed via photodecarboxylation[1,14] and has a high quantum yield in aerated solutions. However, the methylester derivative of MNAA, which cannot undergo direct photodecarboxylation, is also reported to give the aldehyde in aerated acetonitrile as the only product of photodegradation.[14] An explanation for this is the observation that the ester, which shows maximum stability between pH 4−5, is easily cleavable/hydrolyzable in liver homogenate.[15]

Naproxen (6-methoxy-(α-methyl-2-naphthylacetic acid)), on the other hand, induces skin photosensitivity in some patients and also exhibits red blood cells photohemolytic activity and causes photocleavage of DNA.[4,5] Previous literature show that NP may also undergo photodegradation. Flash photolysis studies indicate that NP undergoes photoionization and triplet formation with comparable quantum yield. Decarboxylation of NP leading to a primary-carbon-centered radical was noted in photolysis in air-saturated aqueous buffer.[5] The radical formed then reacts with molecular oxygen, probably yielding a peroxy radical that may induce lipid peroxidation. Alternatively, the carbon-centered radical may react to form 1-(6-methoxy-2-naphthyl) ethanol, which is subject to further oxidation leading to a ketone. The NP photodegradation process is further known to be a source of singlet oxygen,[4,5] that is, NP phototoxicity could arise from formation of superoxide radicals, singlet oxygen, or both. The

* To whom correspondence should be sent. E-mail: leif.eriksson@nat.oru.se.

10.1021/jp805614y CCC: $40.75
Published on Web 10/04/2008

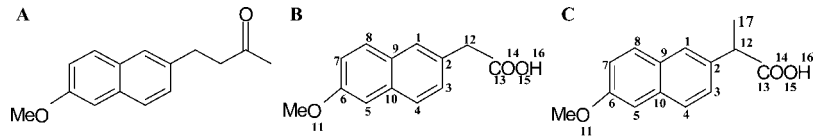

Figure 1. Structure of **A**: NB (4-(6-methoxy-2-naphthyl) butan-2-one); **B**: its active metabolite MNAA (6-methoxy-2-naphthylacetic acid), and **C**: NP (2-(6-methoxy-2-naphthyl)propionic acid).

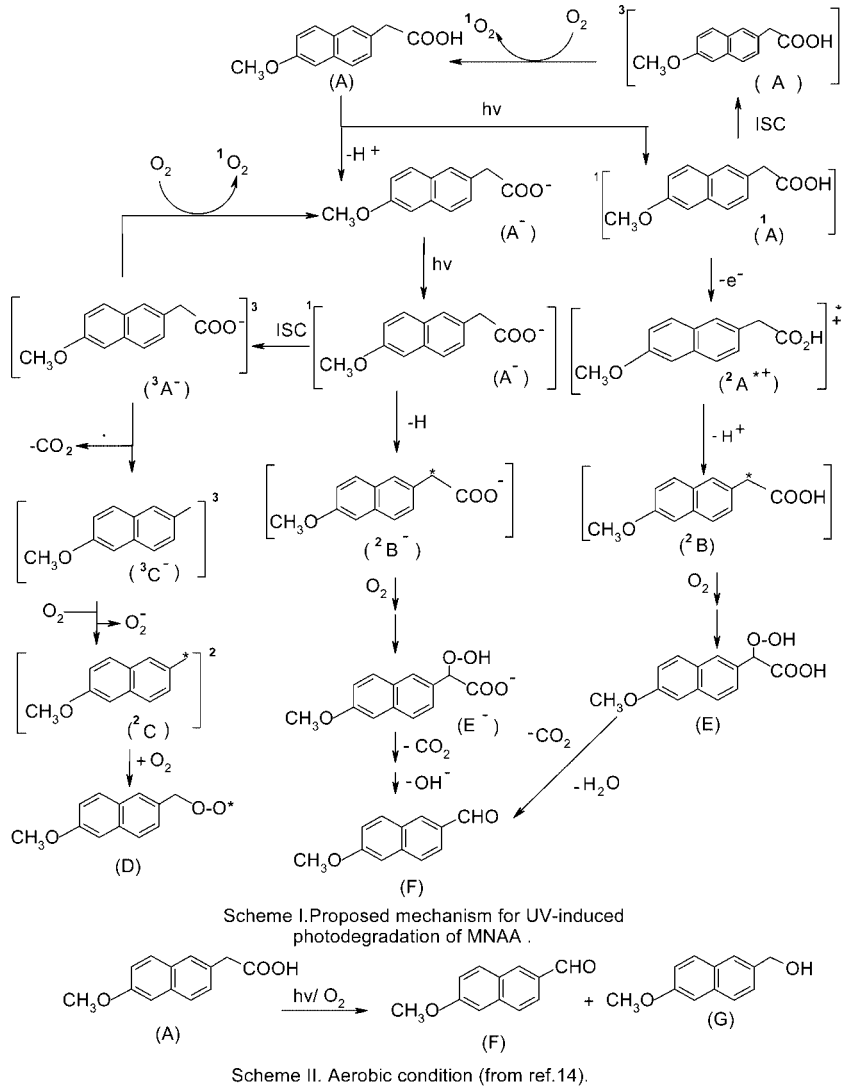

Figure 2. MNAA photodegradation pathways.

different photodegradation pathways are summarized in Figures 2 (MNAA) and 3 (NP).

The pK_a of MNAA should be similar to that of NP, for which values between 3.9 and 4.15 are reported.[16,17] For both of these weak acids, the deprotonated forms will hence dominate under normal physiological conditions. To further understand the photobiological properties and photosensitizing side effects of the active metabolite of nabumetone (MNAA) and of naproxen, we have, in this paper, studied their proposed photodegradation pathways by extensive quantum chemical calculations.

For MNAA, a mechanism involving singlet oxygen, radical formation, and electron transfer reactions have been suggested to account for the observed phototoxicity[18] and forms the basis for one of the pathways explored according to the mechanism shown in Scheme I of Figure 2. The phototoxic reactions of neutral MNAA (**A**) are initiated by the formation of the singlet excited state ^{1}**A** by the absorption of ultraviolet (UV) light. The excited singlet state undergoes one of two possible reactions: either intersystem crossing (ISC) to the triplet state ^{3}**A** or auto-oxidation to form the naphthalene-like radical cation $\mathbf{A}^{\bullet+}$. The triplet state ^{3}**A** can react with an oxygen molecule in its $^3\Sigma$ ground-state to generate singlet oxygen concomitant with relaxation of the triplet state into the initial form **A**. Hence, this route involves a recyclization process that continuously generates singlet oxygen species as a starting process for its phototoxicity.

The electron detachment product $\mathbf{A}^{\bullet+}$ can deprotonate at carbon C_{12} (attached to the naphthalene ring) to form radical **B**. This radical is postulated to react with an oxygen molecule and to lead to the hydroperoxyl form **E,** which in turn may undergo decarboxylation and dehydration to form the aldehyde species **F**.[1,14]

On the basis of the pK_a of the related Naproxen molecule (~4), the above suggested pathways based on neutral MNAA

TABLE 1: B3LYP/6-31G(d,p) ZPE-corrected Electronic Energies in Gas Phase and IEFPCM-B3LYP/6-31G(d,p) Gibbs Free Energies in Aqueous Solution at 298 K[a]

system	$E_{(ZPE)}$	$\Delta E_{(ZPE)}$	ΔG_{aq}^{298}	$\Delta\Delta G_{aq}^{298}$	μ_{aq}
		MNAA			
A (singlet)	−728.094 177	0.0	−728.156 978	0.0	3.30
$\mathbf{A}^{\bullet -}$ (doublet)	−728.083 088	6.96	−728.210 800	−33.77	3.36
$\mathbf{A}^{\bullet +}$ (doublet)	−727.838 250	160.59	−727.961 358	122.75	6.58
$\mathbf{A}^-$ (singlet)	−727.537 688	349.20	−727.685 390	295.93	22.32
$^3\mathbf{A}^-$ (triplet)	−727.460 723	397.49	−727.596 922	351.44	18.56
$^3\mathbf{A}$ (triplet)	−728.006 525	55.00	−728.068 972	55.22	1.83
B (doublet)	−727.471 941	0.0	−727.530 113	0.0	5.97
$\mathbf{B}^-$ (doublet)	−726.909 955	352.65	−727.058 659	295.84	25.20
$^3\mathbf{C}^-$ (triplet)	−538.886 790	0.0	−539.002 271	0.0	4.47
$^2\mathbf{C}$ (doublet)	−538.905 072	−11.47	−538.949 757	32.95	2.30
D (doublet)	−689.247 230		−689.301 950		5.56
E (singlet)	−878.425 909	0.0	−878.500 341	0.0	4.65
$\mathbf{E}^-$ (singlet)	−877.897 057	331.86	−878.039 670	289.08	19.34
F (singlet)	−613.565 469		−613.614 411		5.39
H (singlet)	−614.742 327		−614.797 407		3.01
		NP			
A (singlet)	−767.385 598	0	−767.447 445	0	1.39
$\mathbf{A}^{\bullet -}$ (doublet)	−767.372 696	8.10	−767.500 724	−33.43	2.28
$\mathbf{A}^{\bullet +}$ (doublet)	−767.125 091	163.47	−767.248 389	124.91	6.26
$\mathbf{A}^-$ (singlet)	−766.828 740	349.43	−766.976 620	295.45	20.10
$^3\mathbf{A}^-$ (triplet)	−766.748 091	400.04	−766.880 939	355.49	15.33
$^3\mathbf{A}$ (triplet)	−767.290 221	59.85	−767.354 521	58.31	1.83
B (singlet)	−578.831 763	0	−578.877 999	0	1.41
$^3\mathbf{B}$ (triplet)	−578.737 492	59.16	−578.785 667	57.94	2.01
$\mathbf{B}^-$ (singlet)	−578.215 737	386.56	−578.330 626	343.48	7.28
$^3\mathbf{B}^-$ (triplet)	−578.178 897	409.68	−578.297 189	364.46	2.00
B (doublet)	−578.198 999	397.07	−578.246 900	396.02	1.55
C (singlet)	−654.038 562		−654.094 134		1.52
D (singlet)	−652.865 264		−652.916 142		4.79
E (doublet)	−728.542 990		−728.598 645		4.36

[a] Absolute energies are in a.u., and relative energies are in kcal/mol. Dipole moments μ (debye) in aqueous solution. Compound labels refer to Figures 2 and 3.

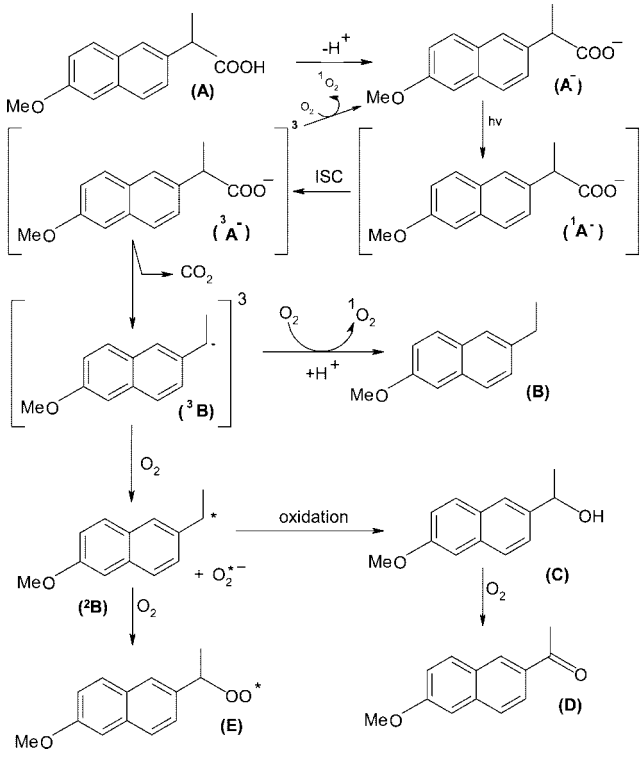

Figure 3. NP photodegradation pathways.

may be considered as less valid. To account for the actual charged form of MNAA under normal physiological conditions, the corresponding pathways for the deprotonated acid $\mathbf{A}^-$ were also explored as follows. Initial excitation leads to the formation of $^1\mathbf{A}^-$, which after ISC to the triplet state $^3\mathbf{A}^-$ can react with an oxygen molecule giving singlet oxygen and regenerate the ground-state singlet. Alternatively, the triplet species may, with high quantum yield (0.29),[19,20] decarboxylate to form $^3\mathbf{C}^-$ and upon electron transfer from $^3\mathbf{C}^-$ serve as a source for superoxide radical anions. The resulting radical $^2\mathbf{C}^\bullet$ can react with another oxygen molecule to give the peroxy radical species $^2\mathbf{D}^\bullet$.

A second possibility for photodegradation of the acid $^1\mathbf{A}^-$ is similar to that of the neutral species, resulting in the formation of $\mathbf{B}^-$ and $\mathbf{E}^-$ and, finally, the aldehyde **F**, which is the common product from both the neutral and the deprotonated pathway. An alternative pathway proposed for MNAA is shown in Scheme II of Figure 2, whereby the photodegradation process under aerobic conditions leads to the formation of the aldehyde **F** and alcohol **G**.[1,14]

To shed more light on this seemingly complex reactivity of MNAA, the mechanistic proposals of Schemes I and II in Figure 2, including several alternative pathways such as the reactivity of the first excited singlet and triplet states of deprotonated MNAA, have been explored using hybrid density functional theory (DFT) methods, time-dependent formalism for the evaluation of vertical excitation energies, UV-absorption spectra. We report optimized structures, distribution of charge and spin in the different species, and the energetics required for their formation.

In previous experimental studies of MNNA, transient absorption spectra were obtained after laser flash excitation at 266 nm of deaerated and aerated solutions of MNAA in acetonitrile (in which the 2-aryl propionic acid-based NSAIDs are normally

neutral). A signal at 440 nm with a lifetime of 4.3 μs was assigned to the triplet state. Another transient with two maxima at 380 and 610 nm and a lifetime of 3.7 μs was assigned to the naphthalene radical cation. Finally, a longer-lived species (25 μs) with a maximum at 340 nm could be associated with the formation of a benzylic radical; however, no further experiments were done to unequivocally confirm the nature of the band. Under oxygen-saturated conditions the signal with maximum at 380 and 610 nm was the only remaining absorption after 1 μs.[14]

When laser flash photolysis of MNAA was performed in PBS solutions, the band at 440 nm assigned to the triplet state showed a 6-times longer lifetime than in acetonitrile (24 μs), whereas the signal with maxima 380 and 610 nm had a lifetime (3.7 μs) similar to that described above. Again, the band at 340 nm (51 μs) was observed, as was a band corresponding to solvated electrons at 710 nm. The same quenching behavior as above was observed in the presence of oxygen. During the triplet state quenching, singlet oxygen is most likely formed, as for the related compounds NP and NB, and with similar quantum yield, $\Phi_\Delta(\sim 0.2)$.[19,20]

The formation of an aldehyde derivative of MNAA in aqueous solution exposed to ultrasound in the dark seems to indicate that in this case OH radicals, which are generated in the process, may catalyze the formation of peroxide radicals in the presence of dissolved oxygen and abstract a hydrogen from the alkyl chain (carbon C_{12}).[1] Formation of an aldehyde under irradiation indicates that the naphthalene radical cation has evolved to a benzylic radical prior to decarboxylation. Trapping of this radical by O_2, subsequent formation of a peroxylactone, and final loss of carbon dioxide (i.e., route $\mathbf{A}^{\bullet+} \rightarrow \mathbf{B} \rightarrow \mathbf{E} \rightarrow \mathbf{F}$ in Figure 2) would explain the formation of the aldehyde.[14]

For NP, the reaction schemes are less complex and largely follow the routes previously outlined for other 2-aryl propionic acid-based NSAIDs such as ibuprofen and ketoprofen.[21,22] These involve excitation of the deprotonated species, intersystem crossing to the first excited triplet, decarboxylation (leading to $^3\mathbf{B}^-$ of Figure 3), and subsequent reactions involving radical quenching or creation of peroxyl radicals.

Computational Details

All calculations were carried out using the GAUSSIAN 03 package,[23] employing the hybrid HF-DFT functional B3LYP [24−26] and the 6−31G(d,p) basis set. At the optimized geometries, zero-point vibrational energies (ZPE) were evaluated, as were free energy corrections at $T = 298$ K. To describe the effect of the surrounding medium, bulk water was included as solvent through single-point calculations at the same level of theory, using the integral equation formalism of the polarized continuum model (IEF-PCM) of Tomasi and co-workers,[27−29] with a ε value of 78.9 for the dielectric constant. Ionization potentials, electron and proton affinities, and excitation energies were obtained at the same level of theory. Atomic charges and spin densities were extracted using Mulliken population analysis. Time dependent DFT (TD-DFT) calculations[30−32] were performed in order to obtain excitation energies and when exploring the possibility for the decarboxylation processes to occur from different excited states. The atomic numbering schemes used for both drugs are given in Figure 1.

Formation of carbon dioxide (the decarboxylation process) was investigated by scanning the $C_{12}-C_{13}$ distance from 1.675 Å in case of MNAA and from 1.733 Å in case of NP in their anionic triplet states and 1.60 Å in the corresponding singlets with step size 0.1 Å. In each point the remaining structural parameters were fully reoptimized.

It is also noteworthy that the current level of theory tends to overestimate excitation energies by approximately 0.2 eV, leading to a blue-shift of the peaks in the computed spectra. Solvent effects have very little influence on the absorptions with the methodology employed herein, and were hence not included in the TD-DFT calculations.

Results and Discussion

A. Redox Chemistry of MNAA and NP. To obtain initial data on the properties of MNAA and NP, their redox chemistries were investigated. In Figures 4 and 5 we display the optimized structures of the neutral ground states (**A**) of MNAA and NP, their radical anions and radical cations ($\mathbf{A}^{\bullet-}$ and $\mathbf{A}^{\bullet+}$), and deprotonated acids ($\mathbf{A}^-$), respectively. The main difference in their optimized structures is a change in $C_{12}-C_{13}$ bond lengths, responsible for decarboxylation, from 1.52 Å in the protonated structures (4A and 5A), to 1.60 Å in the deprotonated forms (4D and 5D), respectively. Very little change is, however, seen in this bond length for the radical anions (4B and 5B) and radical cations (4C and 5C), compared with the neural structure. In these cases, the larger changes are instead found in the methoxy parts.

In Table 1 we list the computed and relative energies of the MNAA and NP species investigated in this study; both the absolute and relative ZPE-corrected energies in gas phase and the absolute and relative Gibbs free energies and dipole moments obtained in aqueous solution. Redox data are, as expected, highly similar for the compounds. Reduction of the neutral species results in a free energy gain of ∼34 kcal/mol in aqueous solution, whereas oxidation requires 123−125 kcal/mol in free energy. In vacuo, the reactions are more endergonic, due to lack of solvent stabilization of the charge species. The small changes in computed dipole moments of the radical anions and radical cations compared with the neutral ground-state molecules (Table 1), and minimal structural effects, can be rationalized in terms of charge delocalization into the naphthalene moiety. The free energy difference between the neutral and deprotonated species (deprotonation free energy) is 295 kcal/mol in aqueous solution. The relative energies are highly similar (to within ca. 10 kcal/mol) to the results obtained for the related NSAIDs ibuprofen and ketoprofen.[21,22]

Mulliken atomic charges and radical spin densities of all species are listed in Supporting Information Tables S1 and S2 for MNAA and Tables S3 and S4 for NP, respectively. The charge localized on the carboxylic moiety of the neutral molecules, radical anions, and radical cations range between +0.04 and −0.22, whereas the methoxy oxygen holds a negative charge of -0.5 ± 0.05 e$^-$ for all species. The unpaired electron is in the radical anions localized to mainly C_1, C_4, C_5, and C_8, with the main component on C_1 (0.30 e$^-$). For radical cations the main component of the charge is found on C_5 (0.28−0.30 e$^-$). The situation is markedly different for the deprotonated acids ($\mathbf{A}^-$), for which the carboxylic groups now hold −0.68 to −0.69 e$^-$ negative charge. This is also reflected in the drastic increase in dipole moments by more than 18 D upon deprotonation. The high charge of the methoxy oxygen (∼−0.5 e$^-$) also remains for these systems.

As noted above, deprotonation leads to an elongation of the $C_{12}-C_{13}$ bond (from 1.52 Å in the neutral species to 1.60 Å). This indicates that decarboxylation may occur more readily once H_{16} is removed. The structural differences, as well the redox chemistry and the differences in photochemical behavior, can

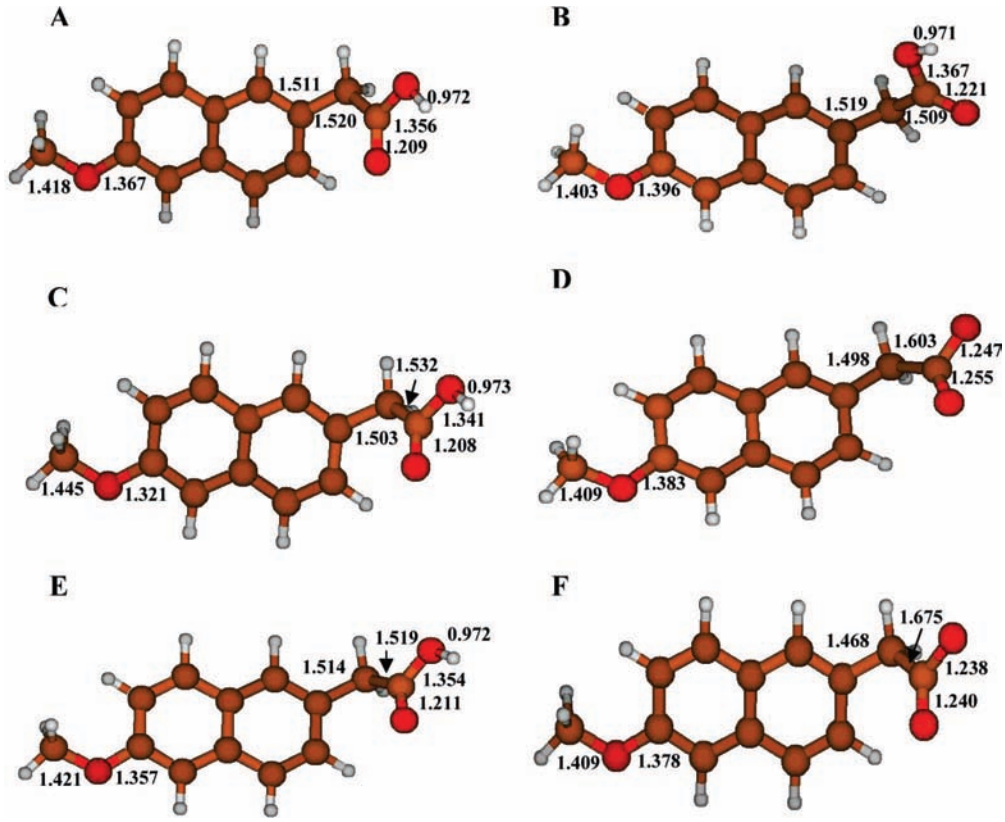

Figure 4. B3LYP/6−31G(d,p) optimized structures of MNAA; (A) neutral ground state (**A**), (B) radical anion ($\mathbf{A}^{\bullet-}$), (C) radical cation ($\mathbf{A}^{\bullet+}$), (D) deprotonated acid ($\mathbf{A}^{-}$), (E) neutral triplet state ($^3\mathbf{A}$), and (F) deprotonated triplet state ($^3\mathbf{A}^{-}$).

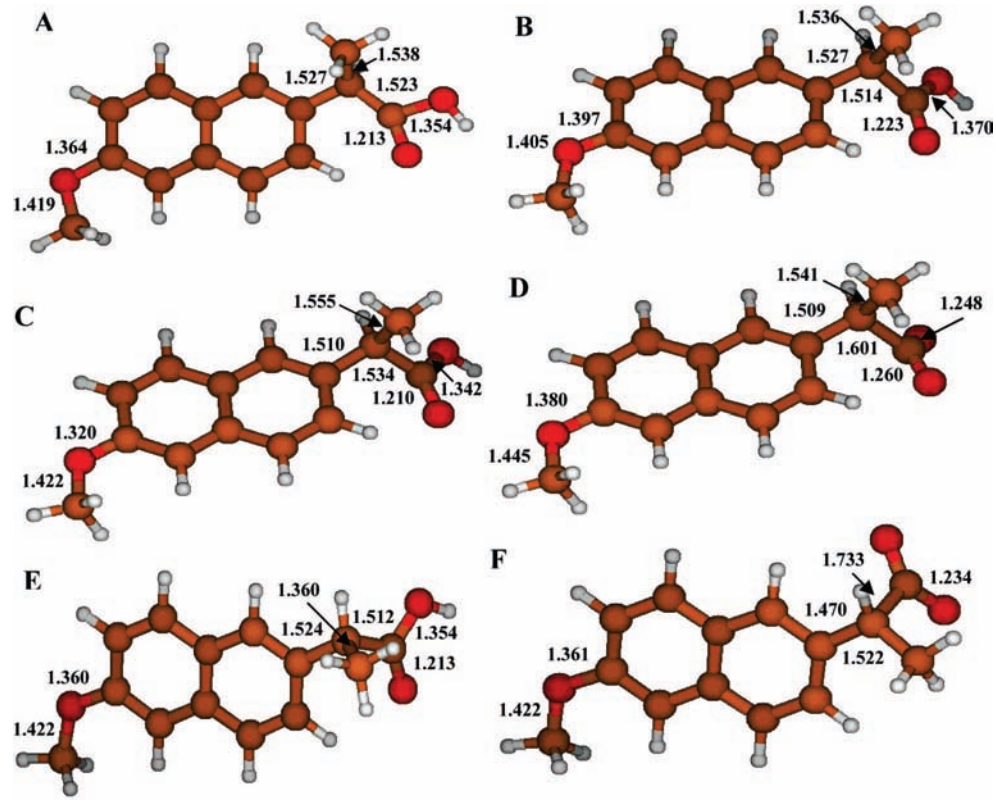

Figure 5. B3LYP/6−31G(d,p) optimized structures of NP; (A) neutral ground state (**A**), (B) radical anion ($\mathbf{A}^{\bullet-}$), (C) radical cation ($\mathbf{A}^{\bullet+}$), (D) deprotonated acid ($\mathbf{A}^{-}$), (E) neutral triplet state ($^3\mathbf{A}$), and (F) deprotonated triplet state ($^3\mathbf{A}^{-}$).

largely be accounted for by considering the highest occupied and lowest unoccupied molecular orbitals (HOMOs and LUMOs), depicted in Figure 6. As seen, the HOMO, HOMO − 1, LUMO, and LUMO + 1 of the neutral species are entirely localized to the naphthalene moieties, as are LUMOs of the acids. Forming the radical anion or cation, hence, only invokes

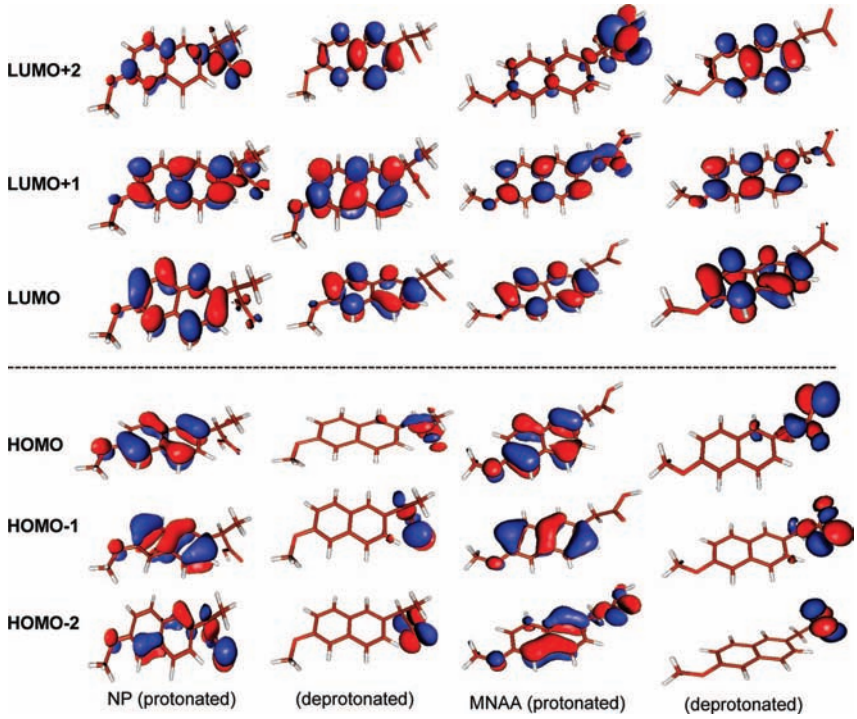

Figure 6. Computed orbitals for NP (left) and MNAA (right).

a slight reorganization of electrons in the conjugated ring system, and thus no drastic changes in the dipole moments are expected (cf. Table 1). Compared with the π-type HOMOs of the protonated species, the HOMOs of the deprotonated compounds are of n-type and are entirely localized on the carboxylic moieties. This accounts for the structural modifications, the large increase in dipole moments, and the considerable differences in the photochemistry between the **A** and $\mathbf{A}^-$ forms of MNAA and NP.

B. Excitation of MNAA and NP and Their Deprotonated Species. The initial step in the photodegradation of MNAA and NP is the excitation of **A**, in its neutral or deprotonated form, to the first excited singlet state S_1 followed by intersystem crossing (ISC) to the first excited triplet state. We display the computed UV-spectra of **A**, $\mathbf{A}^-$, and the decarboxylated form ($^3\mathbf{C}^-$) of MNAA in Figure 7A and of NP in Figure 7B. As seen, the three spectra within each compound are quite different, whereas the corresponding spectra of the two systems are highly similar (e.g., comparing the spectra for the protonated species of MNAA with that for NP).

For MNAA, the first vertical S_1 (HOMO $\rightarrow$ LUMO) excitation of the neutral species occurs at 305 nm (94 kcal/mol), in the UV-regime of spectrum, with an oscillator strength $f = 0.055$, indicative of low probability. The main peak is found at 217 nm with significant oscillator strength 0.58, followed by a small peak at 199 nm. Absorptions are also found at 225 and 215 nm with significantly oscillator strengths (0.34 and 0.46, respectively) appearing as shoulders in the main peak. The S_2 excitation at 277 nm has the lowest oscillator strength (0.01) of all the 10 lowest transitions computed. All the low-lying excitations involve π, π^* transitions from the highest lying occupied MOs to the LUMO.

For the deprotonated species, the lowest lying excitations again occur from the highest occupied MOs to the LUMO, but this time requiring energies about half of those seen for the protonated form. The excitation to the S_1 state is already found at 56 kcal/mol (508 nm), which is well into the visible region,

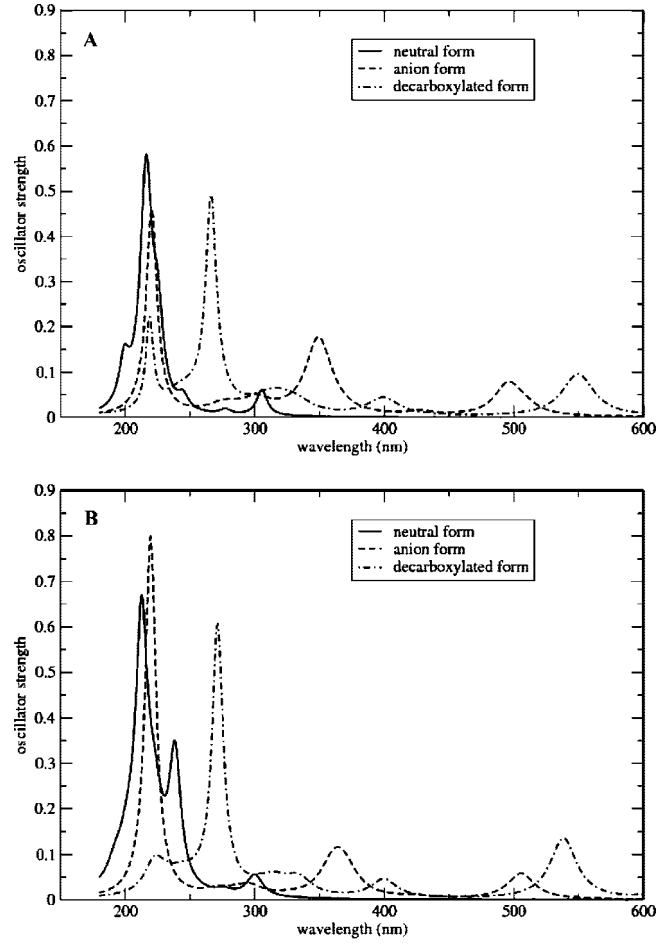

Figure 7. Computed UV-spectra of the neutral (solid), deprotonated (dashed), and decarboxylated (dot-dashed) forms of MNAA (A) and NP (B) at the TD-B3LYP/6−31G(d,p) level.

with oscillator strength 0.008 (i.e., too low of a propability to be detected), followed by several excitations in the visible and

UV parts of the spectrum. The main absorptions occur at 495, 348, 220, and 215 nm with oscillator strengths 0.03, 0.16, 0.46, and 0.03, respectively. As mentioned above, the estimated pK_a of MNAA is around 4, hence we can expect that at physiological pH in aqueous solution the system will be deprotonated. From the data shown herein we can thus expect the species to absorb light in the UV and, to some extent, visible regions. Once the molecule has absorbed light, photodegradation will take place, especially in the case of the anion, where decarboxylation will be the dominant process, and singlet oxygen species and peroxy radical formation are also expected. The computed spectra matches well the experimental data obtained by laser flash photolysis,[14] where the absorption spectrum of MNAA was expected to extend into the biologically relevant UVA−UVB zones due to the presence of the naphthalene chromophore. When the spectrum was measured in acetonitrile and PBS solutions it showed four bands with maxima at 220, 270, 320, and 330 nm.[14] When comparing with the computed spectra, we should also bear in mind the blue-shift frequently observed with the current methodology, giving a shift of the excitations toward shorter wavelengths by approximately 15 nm at $\lambda = 300$ nm, and by 5 nm at $\lambda = 200$ nm.

Addition of a methyl group at position C_{12} of MNAA gives naproxen, the second drug studied herein. This minor change in chemical structure results in a small shift in the position of the absorptions (by ∼10 nm) and slightly higher oscillator strengths, as can be seen in Figure 7. For the neutral species of NP, the first vertical S_1 (HOMO → LUMO) excitation occurs at 299 nm (95.4 kcal/mol), in the UV-regime of spectrum, with an oscillator strength $f = 0.050$, indicative of low probability. The main peak is found at 212 nm, with significant oscillator strength $f = 0.67$. Other main absorptions occur at 238 nm ($f = 0.35$), 220 nm ($f = 0.21$), and 215 nm ($f = 0.14$).

The deprotonated acid of NP shows absorbance peaks in both UV and visible regions of the spectrum. The lowest lying excitations are again from HOMOs to the LUMO, but in this case the excitation to the S_1 state is already found at 505 nm ($f = 0.027$), indicating that NP absorbs radiation stronger than MNAA. The energy required is about half of that seen for the protonated form and is followed by several excitations in the visible and UV parts of the spectrum. The main absorption peak is found at 220 nm ($f = 0.8$). The effects on the spectra, as compared with the corresponding MNAA species, can be related to the electron donating effect of the extra α-mehthyl group present in NP.

The initial $S_0 \rightarrow S_1$ excitation energy of the neutral systems of MNAA (NP) requires 93.6 (95.4) kcal/mol; following ISC to the T_1, this will relax to a free energy 55.2 (58.3) kcal/mol above S_0. For the neutral triplets to deprotonate requires 296.2 (297.3) kcal/mol of energy, that is, very similar to that found for singlet ground-state deprotonation, 295.9 (295. 5) kcal/mol. Excitation to the S_1 state of the deprotonated system requires 55−56 kcal/mol, followed by ISC to $^3\mathbf{A}^-$. The optimized triplet state of the deprotonated form lies 48.3 (50.6) kcal/mol above the optimized ground state ($\mathbf{A}^-$). Alternatively, the systems can be excited to a higher-lying singlet and undergo rapid radiationless decay to S_1 and ISC to T_1. The values are very little affected by the inclusion of bulk solvation. The energies of the optimized deprotonated and neutral triplets agree well with the vertical T_1 energies obtained from TD-DFT calculations of the deprotonated and neutral species; 50 (52) kcal/mol and 60.4 (64) kcal/mol, respectively, indicating that there is very little structural relation of the T_1 state. The experimental value for the T_1 state of MNAA in acetonitrile is 440 nm (62.1 kcal/mol), in prefect agreement with the computed data for the neutral (protonated) form.[14]

In Figures 4 and 5 we display the optimized structures of neutral and deprotonated triplet states ($^3\mathbf{A}$ and $^3\mathbf{A}^-$) for MNAA and NP respectively. For the protonated species, very small changes in geometries are noted, compared with the ground-state forms. In the deprotonated species, the main structural change is an elongation of the $C_{12}-C_{13}$ bond (responsible for the decarboxylation) to 1.675 and 1.733 Å of MNAA and NP, respectively.

The optimized deprotonated triplet states of MNAA (NP) have the main unpaired spin component 0.5 e^- (0.55 e^-) on carbon C_1 on the naphthalene ring and the remainder spread in an alternant fashion throughout the molecule. In the neutral species, the main unpaired spin components 0.54 and 0.52 e^- are found on a carbons C_5 and C_8 on the naphthalene ring of MNAA, whereas for NP the neutral form has its main unpaired spin on carbons C_1 and C_4 with values 0.51 and 0.54 e^-, respectively. MNAA and (NP) have approximately 0.53 (0.50) units of negative charge located on the carboxyl moiety in the optimized triplet state of deprotonated forms, whereas only 0.05 e^- (0.06 e^-) is located on the same group in case of the neutral species. This can also be rationalized from the difference between the HOMO and LUMO of the two forms (neutral and deprotonated) as depicted in Figure 6, leading to an increased possibility for the decarboxylation process to take place from the deprotonated forms rather than from the neutral ones. The radical that is formed after decarboxylation is more stable in NP because the presence of the extra substituent (the α-methyl group). This methyl group has electron donating properties that elongates the bond responsible for decarboxylation and lowers the barrier to decarboxylation. This phenomenon seen for NP is similar to other 2-arylpropionic acid derivatives; ketoprofen decarboxylates spontaneously from its deprotonated triplet state,[21] and in ibuprofen the system only needs to pass a low energy barrier (<0.5 kcal/mol) to decarboxylate from the first excited triplet anion.[22]

To investigate if decarboxylation can occur from the excited singlet states, the $C_{12}-C_{13}$ bond was scanned outward from the optimized value of the deprotonated form of MNAA (NP), 1.603 Å (1.601Å), in steps of 0.1 Å. In each new point the structures were reoptimized, and the vertical excitations calculated. The resulting energy curves, obtained at the TD-B3LYP/6−31G(d,p) level, are displayed in Supporting Information Figures S1 and S2, respectively, which include of ground states and the eight lowest singlet excitations for each system. As expected, the ground and most of the lowest excited singlet state surfaces are strictly endothermic throughout the scan of the $C_{12}-C_{13}$ bond. The exception is for both molecules in the S_4 state which, however, lies rather high in energy (∼80 kcal/mol) and displays a transition barrier at a $C_{12}-C_{13}$ distance of ∼2.4 Å. This barrier is, furthermore, too high (around 24 kcal/mol), and we may conclude that the singlets are unlikely to show any sign of decarboxylation. This situation is markedly different from the case of ketoprofen, for which several of the singlet excited states of the deprotonated form would lead to decarboxylation by overcoming a barrier of only a few kcal/mol.[21] In that sense, both MNAA and NP display a reactivity more similar to that found for ibuprofen.[22]

To determine the energy barrier required for decarboxylation from the triplet state of the deprotonated form of MNAA (NP), scans of the $C_{12}-C_{13}$ distance were performed in steps of 0.1 Å, starting from the bond length obtained from the triplet state optimizations; 1.675 Å (1.733 Å). The results are depicted in

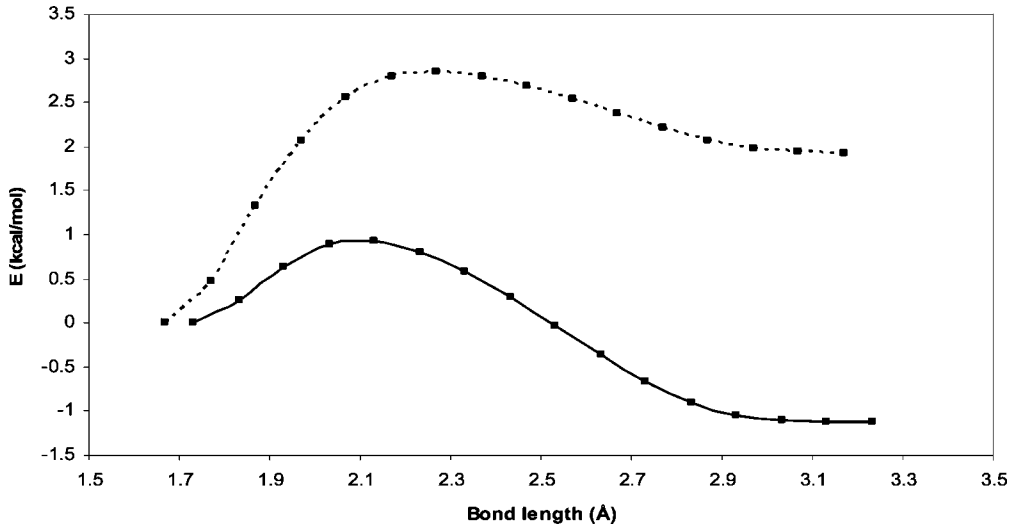

Figure 8. Reaction path for decarboxylation of $^3\mathbf{A}^-$ to produce $^3\mathbf{C}^-$ of MNAA (dashed line) and $^3\mathbf{B}^-$ of NP (solid line).

Figure 8 and show that there are very low energy barriers, only 2.8 (0.9) kcal/mol, toward decarboxylation. The $C_{12}-C_{13}$ transition state distance is approximately 2.25 (2.13) Å. We note that the reaction of MNAA is endothermic, whereas that of NP is exothermic. These results are consistent with previous discussions on the electron-donating properties of the extra methyl group in NP, assisting both in the dissociation of the CO_2 moiety and in stabilizing the resulting open shell species.

C. Photodegradation Mechanism of MNAA. The photodegradation pathways of MNAA intermediates depicted in Figure 2 can be summarized as reactions 1−5 in addition to reaction 9. Reactions 1 and 2 involve the neutral molecule ($^1\mathbf{A}$), reactions 3−5 show the fate of the deprotonated form, and reaction 9 applies to oxygen-rich conditions.

$$\mathbf{A} \xrightarrow{h\nu} {}^1\mathbf{A} \xrightarrow{\mathrm{ISC}} {}^3\mathbf{A} \xrightarrow{+O_2} \mathbf{A} + {}^1O_2 \qquad (1)$$

$$\mathbf{A} \xrightarrow{h\nu} {}^1\mathbf{A} \xrightarrow{-e} {}^2\mathbf{A}^{\bullet+} \xrightarrow{-H^+} {}^2\mathbf{B} \xrightarrow{O_2} \rightarrow \mathbf{E} \xrightarrow[-H_2O]{-CO_2} \mathbf{F} \qquad (2)$$

Reaction 1 shows the photoinduced generation of singlet oxygen, in which the neutral form of MNAA (**A**) is excited to the first excited singlet state by exposure to UV-light (ΔE = 94 kcal/mol), followed by ISC to the T_1 state ($^3\mathbf{A}$) located about 48 kcal/mol below the excited singlet. It is noteworthy that this poses a very large energy gap between S_1 and T_1, indicative of the low quantum yield of the process. Once the triplet state is formed it will, in the presence of molecular oxygen, lead to singlet oxygen formation (which constitutes a vital component of phototoxic side effects of the drug) and regenerates the starting parent molecule, thus serving as a recycling process for singlet oxygen generation. The excitation energy of molecular oxygen is only 22.7 kcal/mol,[33] and hence very feasible from the T_1 state.

Reaction 2 outlines the fate of the singlet excited-state through a redox mechanism. The electron detachment energy lies 160 kcal/mol above the singlet excited-state in the gas phase. Bulk solvation stabilizes the oxidized species by 38 kcal/mol. Deprotonation from the carbon atom attached directly to the naphthalene ring (C_{12}) renders radical $^2\mathbf{B}$, with a deprotonation free energy as high as 270.6 kcal/mol. C_{12} holds the main component of the unpaired spin (0.59 e^-) and is susceptible to react with molecular oxygen, leading to the ground-state peroxy form **E.** This may undergo decarboxylation followed by dehydration at carbon C_{12}, leading to the formation of aldehyde **F**.

The deprotonated form of MNAA may undergo several pathways as follows.

$$\mathbf{A}^- \xrightarrow{h\nu} {}^1\mathbf{A}^- \xrightarrow{\mathrm{ISC}} {}^3\mathbf{A}^- \xrightarrow{+O_2} \mathbf{A}^- + {}^1O_2 \qquad (3)$$

$$\mathbf{A}^- \xrightarrow{h\nu} {}^1\mathbf{A}^- \xrightarrow{\mathrm{ISC}} {}^3\mathbf{A}^- \xrightarrow{-CO_2} {}^3\mathbf{C}^- \xrightarrow{O_2} O_2^{*-} + {}^2\mathbf{C} \xrightarrow{O_2} \mathbf{D}(OO^{\bullet}) \qquad (4)$$

$$\mathbf{A}^- \xrightarrow{h\nu} {}^1\mathbf{A}^- \xrightarrow{-H} \mathbf{B}^- \xrightarrow{O_2} \rightarrow \mathbf{E}^- \xrightarrow[-OH]{-CO_2} \mathbf{F} \qquad (5)$$

Reactions 3 and 5 are similar to those outlined for the neutral form. Accordingly, in reaction 3 the deprotonated form of MNAA ($\mathbf{A}^-$) is excited to the first excited singlet state ($^1\mathbf{A}^-$),which requires ca. 55 kcal/mol of energy. After ISC, the triplet state ($^3\mathbf{A}^-$) is formed, located about 48 kcal/mol above the singlet ground state. In the presence of molecular oxygen, this can be excited in a radiationless process by the triplet giving singlet oxygen (energy required to excite ground-state oxygen is 22.7 kcal/mol[33]), whereby the MNAA acid relaxes to its ground state.

After ISC, another possibility exists as shown in reaction 4. In this case the triplet state decarboxylates by passing over a low energy barrier (see Figure 8). The electron affinity of molecular oxygen in aqueous solution is 90.2 kcal/mol,[34] and hence, by electron transfer to oxygen to form the superoxide radical, the endothermic energy difference between $^3\mathbf{C}^-$ and $^2\mathbf{C}$ (33 kcal/mol) is readily overcome. $^2\mathbf{C}$ possesses significant unpaired spin density on carbon atom C_{12} (0.73 e^-), making this site very reactive and thus readily forms a bond with a second oxygen molecule in its ground state, leading to peroxy radical **D**. This will be capable of abstracting a hydrogen atom from a lipid molecule, reaction 6, which in turn will add molecular oxygen to the new $\mathbf{L}^{\bullet}$ radical site, thereby creating a propagating radical damage. Once initiated, chain reactions 7 and 8 will repeat until terminated by for example, radical−radical addition or the action of a lipid-soluble antioxidant such as vitamin E.

$$^2\mathbf{D}(OO^{\bullet}) + \mathbf{L}H \rightarrow \mathbf{D}(OOH) + \mathbf{L}^{\bullet} \qquad (6)$$

$$\mathbf{L}^{\bullet} + O_2 \rightarrow \mathbf{L}OO^{\bullet} \qquad (7)$$

$$\mathbf{LOO^{\bullet}} + \mathbf{LH} \rightarrow \mathbf{LOOH} + \mathbf{L^{\bullet}} \quad (8)$$

The final proposed pathway for the deprotonated form, reaction 5, involves hydrogen atom abstraction from C_{12} whereby $\mathbf{B}^-$ is formed. The radical anion form possesses its main unpaired spin density at the site of hydrogen abstraction (0.629 e^-), which is higher than for the corresponding form of the neutral pathway (0.591 e^-). The energy difference between the neutral and deprotonated forms of **B** are highly similar to those of the parent compounds **A** and $\mathbf{A}^-$. $^2\mathbf{B}^-$ has a very reactive site at C_{12} that can readily react with molecular oxygen, leading to formation of $\mathbf{E}^-$. Similar to the neutral form, $\mathbf{E}^-$ undergoes decarboxylation, leading to formation of aldehyde **F.**

The last route of photodegradation of MNAA has been proposed to occur in an oxygen-rich environment (Figure 2, Scheme II), reaction 9, whereby the neutral form **A**, upon exposure to UV radiation in presence of oxygen, will be degraded into the aldehyde **F** and the alcohol **G.**

$$\mathbf{A} \xrightarrow[O_2]{h\upsilon} \mathbf{G} + \mathbf{F} \quad (9)$$

Irradiation of MNAA in aerated PBS aqueous solution lead to the formation **G** and **F** as major photoproducts, and the same photoproducts were obtained in aerated acetonitrile.[2] As seen from the computed UV spectra, the neutral form of MNAA predominates under these conditions, which explains why the photodecarboxylation quantum yield was 100 times higher under aerated than deaerated conditions.[35] The mechanism that would operate in addition to direct decarboxylation involves oxidation, deprotonation of the naphthalene radical cation leading to a "nondecarboxylated" naphthylic radical intermediate that will be trapped by O_2. Subsequent formation of a peroxylactone and final loss of carbon dioxide through oxidative fragmentation would explain the formation of aldehyde **F** (Figure 2, Scheme I).[14] The formation of an aldehyde under these irradiation conditions hence indicates that the naphthalene radical cation has evolved to the naphthylic radical prior to decarboxylation.

D. Photodegradation Mechanism of NP. For NP, the chemistry involved is more straightforward due to the electron-donating effect of the additional methyl group, which enhances decarboxylation of the acid once excited to the T_1 state. Once decarboxylation has occurred, the resulting molecule $^3\mathbf{B}^-$ may undergo several reactions, as indicated in Figure 3. The first possibility is reaction 10, in which protonation of radical anion $^3\mathbf{B}^-$ takes place, leading to formation of the ethyl derivative **B.** The proton affinity of $^3\mathbf{B}^-$ is 307.5 kcal/mol in aqueous solution (Table 1). $^3\mathbf{B}^-$ will not be capable of generating $^1O_2$ directly, as the $^3\mathbf{B}^- - {}^1\mathbf{B}^-$ energy difference is 21 kcal/mol, which is lower than the energy required for excitation of ground-state molecular oxygen (22.7 kcal/mol). Once protonated, however, $^3\mathbf{B}$ will readily form $^1O_2$ by decay to the ^{1}B ground state (ΔG ~58 kcal/mol).

Reaction 11 is another possible pathway of the decarboxylated species, in which $^3\mathbf{B}^-$ reacts with molecular oxygen, leading to the formation of superoxide radical anion and the radical ^{2}**B.** This reaction is exergonic by ~59 kcal/mol and hence a very viable step. The doublet may in turn react with another molecule of oxygen that, due to the spin density mainly being located on C_{12} (0.72 e^-), leads to formation of the corresponding peroxy radical **E.** Compound **E** will be capable of initiating lipid peroxidation processes[4] by the same route mentioned for MNAA; reactions 6−8.

$$^3\mathbf{B}^- \xrightarrow[O_2]{H^+ \text{ shift}} \mathbf{B} + {}^1O_2 \quad (10)$$

$$^3\mathbf{B}^- \xrightarrow[OH^-]{+O_2} {}^2\mathbf{B} + O_2^{\bullet -} \xrightarrow{+O_2} \mathbf{E} \quad (11)$$

$$^2\mathbf{B} \xrightarrow{+O_2} {}^1O_2 + \mathbf{C} \xrightarrow{+O_2} \mathbf{D} \quad (12)$$

The last reaction in this scenario is reaction 12, according to which the doublet ^{2}**B**, once formed, will react with oxygen and water to give the 6-methoxy-2-naphthylethanol form (**C**), that upon further oxidation will yield 2-acetyl-6-methoxynaphthalene (**D**).[4] The site of the alcohol or ketone functinal group will be C_{12}; the reactive radical site of ^{2}**B**.

Conclusions

The properties and photochemical degradation mechanisms of the two closely related NSAIDs naproxen and the active form of nabumetone (MNAA) were studied theoretically at the DFT/B3LYP 6−31G (d,p) level of theory. From experimental data available in the literature, the pK_a values of NP and MNAA should lie in the range 3.9−4.15, and hence the deprotonated forms will dominate under physiological pH.

The optimized structures of MNAA and NP show that there are a very few differences in bond lengths of the neutral species, the radical anion, the radical cation, and the deprotonated acid in their singlet ground states. The only significant difference is noted for the $C_{12}-C_{13}$ bond length (responsible for decarboxylation) for the acids, which increase by ~0.08 Å. In the optimized triplet states of the deprotonated acids this increases further, to 1.675 Å (MNAA) and 1.733 Å (NP). The difference seen between the two compounds can be related to the electron donating effect of the additional α-methyl group present in NP.

The extra methyl group also further influences the reactivity and photochemistry. Scanning the $C_{12}-C_{13}$ bond in the singlet and triplet states of the deprotonated acids shows that the decarboxylation will not occur from their excited singlet states. For the triplet states, decarboxylation can instead occur with high efficiency given the low energy barriers of less than 3 kcal/mol (MNAA) and 1 kcal/mol (NP). Noteworthy is the higher barrier and that the decarboxylation is endothermic for MNAA, as this lacks the stabilizing methyl group.

The presence of the methyl group does, however, only render minor differences in the computed UV and visible absorption spectra of MNAA versus NP forms in their neutral, deprotonated, and decarboxylated forms, both regarding the shapes and the positions of the peaks. The only notable trend is that the oscillator strengths are slightly higher for the absorptions of the NP derivatives.

Singlet oxygen, superoxide radical anions, and peroxylic radical species are expected to be formed in different steps throughout the photodegradation pathways of both drugs, which subsequently will produce their action on biomolecules, including the initiation of propagating lipid peroxidation reactions.

Taking into account that most of the phototoxic action occurs after decarboxylation, we conclude that NP is more phototoxic than MNAA. The presence of the additional, electron donating, α-methyl group results in a larger elongation of the $C_{12}-C_{13}$ bond length, which is responsible for decarboxylation, in the optimized triplet state of deprotonated NP relative to that found in MNAA. Decarboxylation is furthermore associated with a ca. 2 kcal/mol lower energy barrier for NP than MNAA and renders a more stable resulting open shell species. Of importance is also the notable fact that we, by comparison between

experimental and theoretical spectra, can conclude that the experiments are performed on neutral MNAA; similar observations have been noted also for other NSAIDs, and it appears that acetonitrile and PBS are less suitable solutions for the study of the photochemistry of these compounds.

Acknowledgment. The MENA programme (KAKM), the Faculty of Science and Technology at Örebro University, and the Swedish Science Research Council (LAE) are gratefully acknowledged for financial support. We also acknowledge generous grants of computing time at the National Supercomputing Center (NSC) in Linköping.

Supporting Information Available: Additional materials mentioned in the text is separately provided. This material is available free of charge via the Internet at http://pubs.acs.org.

References and Notes

(1) Valero, M.; Costa, S. M. B. Photodegradation of Nabumetone in aqueous solutions. *J. Photochem. Photobiol. A-Chem.* **2003**, *157*, 93–101.

(2) Pulgarin, J. A. M.; Molina, A. A.; Robles, I. S. F. Simple and rapid determination of the active metabolite of nabumetone in biological fluids by heavy atom-induced room temperature phosphorescence. *Anal. Chim. Acta* **2005**, *554*, 37–42.

(3) Hedner, T.; Samulesson, O.; Wahrborg, P.; Wadenvik, H.; Ung, K. A.; Ekbom, A. Nabumetone—Therapeutic use and safety profile in the management of osteoarthritis and rheumatoid arthritis. *Drugs* **2004**, *64*, 2315–2343.

(4) Partyka, M.; Au, B. H.; Evans, C. H. Cyclodextrins as phototoxicity inhibitors in drug formulations: studies on model systems involving naproxen and beta-cyclodextrin. *J. Photochem. Photobiol. A-Chem.* **2001**, *140*, 67–74.

(5) Jimenez, M. C.; Miranda, M. A.; Tormos, R. Photochemistry of naproxen in the presence of β-cyclodextrin. *J. Photochem. Photobiol.* **1997**, *104*, 119–121.

(6) Ashworth, N. L.; Peloso, P. M.; Muhajarine, N.; Stang, M. Risk of hospitalization with peptic ulcer disease or gastrointestinal hemorrhage associated with nabumetone, Arthrotec((R)), diclofenac, and naproxen in a population based cohort study. *J. Rheum.* **2005**, *32*, 2212–2217.

(7) Ishiwata, Y.; Okamoto, M.; Yokochi, S.; Hashimoto, H.; Nakamura, T.; Miyachi, A.; Naito, Y.; Yoshikawa, T. Non-steroidal anti-inflammatory drug nabumetone, prevents indometacin-induced gastric damage via inhibition of neutrophil functions. *J. Pharm. Pharmacol.* **2003**, *55*, 229–237.

(8) Arai, Y.; Tanaka, K. I.; Ushijima, H.; Tomisato, W.; Tsutsumi, S.; Aburaya, M.; Hoshino, T.; Yokomizo, K.; Suzuki, K.; Katsu, T.; Tsuchiya, T.; Mizushima, T. Low direct cytotoxicity of nabumetone on gastric mucosal cells. *Dig. Dis. Sci.* **2005**, *50*, 1641–1646.

(9) Nobilis, M.; Kopecky, J.; Kvetina, J.; Svoboda, Z.; Pour, M.; Kunes, J.; Holcapek, M.; Kolarova, L. Comparative biotransformation and disposition studies of nabumetone in humans and minipigs using high-performance liquid chromatography with ultraviolet, fluorescence and mass spectrometric detection. *J. Pharm. Biomed. Anal.* **2003**, *32*, 641–656.

(10) Drugs.com, Drug Information Online, http://www.drugs.com/pdr/NABUMETONE.html.

(11) Reitblat, T.; Zamir, D.; Estis, L.; Priluk, R.; Drogenikov, T.; Viskoper, J. R. The different patterns of blood pressure elevation by rofecoxib and nabumetone. *J. Hum. Hypertens.* **2002**, *16*, 431–434.

(12) Krischer, J.; Scolari, F.; Kondo-Oestreicher, M.; Vollenweider-Roten, S.; Saurat, J. H.; Pechere, M. Pseudoporphyria induced by nabumetone. *J. Am. Acad. Dermatol.* **1999**, *40*, 492–493.

(13) Magro, C. M.; Crowson, A. N. Pseudoporphyria associated with Relafen therapy. *J. Cutan. Pathol.* **1999**, *26*, 42–47.

(14) Bosca, F.; Canudas, N.; Marin, M. L.; Miranda, M. A. A photophysical and photochemical study of 6-methoxy-2-naphthylacetic acid, the major metabolite of the phototoxic nonsteroidal antiinflammatory drug nabumetone. *J. Photochem. Photobiol.* **2000**, *71*, 173–177.

(15) Wadhwa, L. K.; Chandiran, S.; Sharma, P. D. Alkyl esters of 6-methoxy-2-naphthylacetic acid as potential prodrugs -synthesis, physicochemical properties, chemical stability and enzymatic hydrolysis. *Indian J. Chem.* **2004**, *43B*, 1292–1298.

(16) Foye, W. O. *Principios de Química Farmacéutica*, 2nd ed.; Reverté: Spain, 1984.

(17) www.drugbank.ca/drugs/DB00788.

(18) Canudas, N.; Zamora, D.; Villamizar, J. E.; Fuentes, J.; Castelli, C.; Taddei, A. Photosensitizing properties of 6-methoxy-2-naphthylacetic acid, the major metabolite of the phototoxic non-steroidal anti-inflammatory and analgesic drug nabumetone. *Pharmazie* **2005**, *60*, 604–608.

(19) Martinez, L. J.; Scaiano, J. C. Characterization of the transient intermediates generated from the photoexcitation of nabumetone: A comparison with naproxen. *J. Photochem. Photobiol.* **1998**, *68*, 646–651.

(20) De La Pena, D.; Marti, C.; Nonell, S.; Martinez, L. A.; Miranda, M. A. Time-resolved near infrared studies on singlet oxygen production by the photosensitizing 2-arylpropionic acids. *J. Photochem. Photobiol.* **1997**, *65*, 828–832.

(21) Musa, K. A. K.; Matxain, J. M.; Eriksson, L. A. Mechanism of Photoinduced Decomposition of Ketoprofen. *J. Med. Chem.* **2007**, *50*, 1735–1743.

(22) Musa, K. A. K.; Eriksson, L. A. Theoretical study of ibuprofen phototoxicity. *J. Phys. Chem. B.* **2007**, *111*, 13345–13352.

(23) Frisch, M. J.; Trucks, G. W.; Schlegel, H. B.; Scuseria, G. E.; Robb, M. A.; Cheeseman, J. R.; Montgomery, J. A., Jr.; Vreven, T.; Kudin, K. N.; Burant, J. C.; Millam, J. M.; Iyengar, S. S.; Tomasi, J.; Barone, V.; Mennucci, B.; Cossi, M.; Scalmani, G.; Rega, N.; Petersson, G. A.; Nakatsuji, H.; Hada, M.; Ehara, M.; Toyota, K.; Fukuda, R.; Hasegawa, J.; Ishida, M.; Nakajima, T.; Honda, Y.; Kitao, O.; Nakai, H.; Klene, M.; Li, X.; Knox, J. E.; Hratchian, H. P.; Cross, J. B.; Bakken, V.; Adamo, C.; Jaramillo, J.; Gomperts, R.; Stratmann, R. E.; Yazyev, O.; Austin, A. J.; Cammi, R.; Pomelli, C.; Ochterski, J. W.; Ayala, P. Y.; Morokuma, K.; Voth, G. A.; Salvador, P.; Dannenberg, J. J.; Zakrzewski, V. G.; Dapprich, S.; Daniels, A. D.; Strain, M. C.; Farkas, O.; Malick, D. K.; Rabuck, A. D.; Raghavachari, K.; Foresman, J. B.; Ortiz, J. V.; Cui, Q.; Baboul, A. G.; Clifford, S.; Cioslowski, J.; Stefanov, B. B.; Liu, G.; Liashenko, A.; Piskorz, P.; Komaromi, I.; Martin, R. L.; Fox, D. J.; Keith, T.; Al-Laham, M. A.; Peng, C. Y.; Nanayakkara, A.; Challacombe, M.; Gill, P. M. W.; Johnson, B.; Chen, W.; Wong, M. W.; Gonzalez, C.; Pople, J. A. *Gaussian 03*, rev. B.02; Gaussian, Inc.: Wallingford, CT, 2004.

(24) Becke, A. D. Density-functional thermochemistry. 3. The role of exact exchange. *J. Chem. Phys.* **1993**, *98*, 5648–5652.

(25) Stephens, P. J.; Devlin, F. J.; Chabalowski, C. F.; Frisch, M. J. Ab Initio Calculation of vibrational absorption and circular dichroism spectra using density functional force fields. *J. Phys. Chem.* **1994**, *98*, 11623–11627.

(26) Lee, C.; Yang, W.; Parr, R. G. Development of the Colle-Salvetti correlation-energy formula into a functional of the electron density. *Phys. Rev.* **1988**, *37*, 785.

(27) Mennucci, B.; Tomasi, J. Continuum solvation models: A new approach to the problem of solute's charge distribution and cavity boundaries. *Chem. Phys.* **1997**, *106*, 5151–5158.

(28) Cossi, M.; Scalmani, G.; Rega, N.; Barone, V. New developments in the polarizable continuum model for quantum mechanical and classical calculations on molecules in solution. *J. Chem. Phys.* **2002**, *117*, 43–54.

(29) Cances, E.; Mennucci, B.; Tomasi, J. A new integral equation formalism for the polarizable continuum model: Theoretical background and applications to isotropic and anisotropic dielectrics. *J. Chem. Phys.* **1997**, *107*, 3032–3041.

(30) Bauernschmitt, R.; Ahlrichs, R. Treatment of electronic excitations within the adiabatic approximation of time dependent density functional theory. *Chem. Phys. Lett.* **1996**, *256*, 454–464.

(31) Casida, M. E.; Jamorski, C.; Casida, K. C.; Salahub, D. R. Molecular excitation energies to high-lying bound states from time-dependent density-functional response theory: Characterization and correction of the time-dependent local density approximation ionization threshold. *J. Chem. Phys.* **1998**, *108*, 4439–4449.

(32) Stratmann, R. E.; Scuseria, G. E.; Frisch, M. J. An efficient implementation of time-dependent density-functional theory for the calculation of excitation energies of large molecules. *J. Chem. Phys.* **1998**, *109*, 8218–8224.

(33) Huber, K. P.; Herzberg, G. *Molecular Spectra and Molecular Structure 4: Constants of Diatomic Molecules*; van Nostrand, N. Y., 1979.

(34) Llano, J.; Raber, J.; Eriksson, L. A. Theoretical study of phototoxic reactions of psoralens. *J. Photochem. Photobiol. A-Chem.* **2003**, *154*, 235–243.

(35) Moore, D. E.; Chappuis, P. P. A comparative study of the photochemistry of the non-steroidal anti-inflammatory drugs, naproxen, benoxaprofen and indomethacin. *J. Photochem. Photobiol.* **1988**, *47*, 173–180.

JP805614Y